COMPARATIVE STUDY OF INLET MANIFOLD TUNING TO ENHANCE SUPERCHARGE

Mtui P L
Institute of Production Innovation
University of Dar es Salaam

Abstract

Computer modeling and experimental results on a single cylinder, four-stroke cycle engine for best air flow characteristic is discussed. The modeling analysis is based on hometropic fluid flow with constant specific heats. The modeling results is included to validate the simulation program against experimental results with widely varying manifold lengths and engine speeds.

Experimental results are obtained by measuring air flow rates to the inlet valve during steady state speed of the engine. Manifold tuned lengths are obtained for a range of speeds by experiment and by computer simulation, whose results are compared with those obtained using Helmholtz resonator theory of manifold tuning.

1.0 Introduction

Since the modern first engine was introduced in 1876, efforts have been invested in the design of proper manifolds, especially so, for the four-stroke cycle engines. The gas exchange during the inlet and exhaust processes contributes towards the performance of the reciprocating engines. The non steady gas flow in the piping system results in the propagation of pressure waves in the manifolds which may considerably improve (ramming effect) or seriously distort (poor scavenging) the gas exchange process.

A number of mathematical models have emerged to analyze the formation and propagation of these waves aiming at predicting engine performance. Before the introduction of computers, a graphical[7] method was used for the solution of the characteristic equations. With the introduction of digital computers, algorithms have replaced the graphical method.

Ramming effect to improve engine performance has long been studied[4]. Engine design for this effect has largely depended on empirical relationship for the determination of proper manifold lengths. Since four stroke cycle engines are known to be more sensitive to intake conditions than exhaust conditions, an attempt to improve volumetric efficiency is approached by inlet manifold tuning.

The mathematical modeling used in this analysis assumes hometropic, unsteady one-dimensional flow without area change in the duct. The modeling algorithm is written in Fortran 77 for computer application. A single cylinder four-stroke cycle engine is used to demonstrate the application of the modeling. The simulation results are validated against the experimental findings.

In the efforts to utilize the "ramming" effect for better cylinder filling, the tuned lengths are obtained by applying acoustic theory based on Helmholtz resonator model. All the results are compared and analyzed aiming at improving air flow characteristics in the engine.

2.0 Engine Gas Exchange

2.1 Volumetric Efficiency of Four-Stroke Cycle Engine

The ramming effect in engine has long been recognized though has not yet been accurately incorporated in engine at wide range of speeds. The ramming effect is considered in conjunction with the basic theory of sound and its energy in relation with what occurs in the engine piping system so as to utilize this effect for better cylinder filling. There are two models found in literature so far which explain the resonance effect; namely organ pipe theory and Helmholtz resonance theory.

2.1.1 Organ Pipe Theory

This type of resonance (closed pipe end) is utilized by having a multiple integer of organ pipe oscillations within the complete engine cycle.

2.2.2 Helmholtz Resonator

Helmholtz pipe resonance theory relies entirely on a different principle from the organ pipe theory. For Helmholtz resonance every oscillation is initiated and utilized during that particular inlet stroke and thus there is no dependence of one inlet stroke over the result of the previous one. This phenomenon gives rise to a distinct difference in the type of manifold tuning obtained from the two categories. The resonant frequency is given by

$f_o = \frac{a}{2\pi} \frac{A}{\sqrt{LV_c}}$. When applied to the engine cylinder, the cylinder volume is that at the mid stroke i.e one half displacement plus the clearance volume.

Thus $V_{eff} = \frac{V_c}{2} \frac{(CR + 1)}{(CR - 1)}$ where V_c above is replaced by V_{eff}.

When the engine is in operation, the Helmholtz oscillation is initiated by the movement of the piston on the gas intake stroke since the vacuum in the cylinder accelerates the mass of air in the pipe to cylinder. After the pressure falls below atmospheric (Fig 2.1) which in practice occurs approximately at the mid stroke, the pressure rises sinusoidally to a peak at a time determined by Helmholtz frequency.

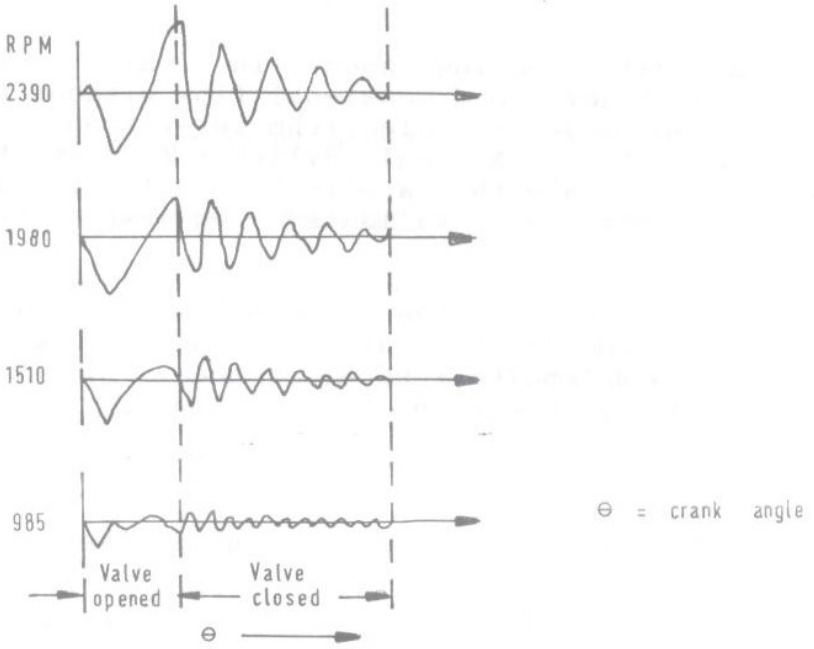

Fig 2.1 Pressure-time history at four engine speeds[4]

Now if the intake valve closes at any time while the pressure in the cylinder is above atmospheric, then supercharge will occur. From this process it is clear that the phenomenon which potentially gives the largest increase in breathing capacity of an engine is the Helmholtz type of resonance.

3.0 Modeling Theory

3.1 Unsteady Flow Modeling

The propagation of pressure waves along the engine pipe system in response to events inside the cylinder as the valves close and open is the basic process which determines the engine breathing behavior. In hometropic flow, this process can be modeled mathematically by the three conservation equations which govern the one dimensional, unsteady compressible fluid flow:

Continuity $$\frac{1}{\rho}\frac{\partial \rho}{\partial t} + \frac{u}{\rho}\frac{\partial \rho}{\partial x} + \frac{\partial u}{\partial x} = 0 \qquad (3.1)$$

Momentum $$\frac{1}{\rho}\frac{\partial p}{\partial x} + \frac{\partial u}{\partial t} + u\frac{\partial u}{\partial x} = 0 \qquad (2.2)$$

Constant entropy $$\frac{p}{p_{ref}} = \left[\frac{a}{a_{ref}}\right]^{2\gamma/(\gamma-1)} \qquad (3.3)$$

Since there is no analytical method of solution for the above conservation equations so far, they are then rearranged and transformed into a set of ordinary differential equations and solved by numerical technique based on the method of characteristics. This method relies upon finding certain characteristic directions in the flow field along which the discontinuities in the derivatives of the fluid properties may propagate.

The procedure for the solution in question is that the pipe is segmented into a number of equal lengths and the calculations are advanced in a series of time steps. At each mesh point, if required, the thermodynamic parameters of interest can be evaluated in the time-space grid. Through this way the motion resulting from the superposition of left moving and right moving

pressure waves can be calculated over the cylinder and manifold system. Thus, along curve of slopes of wave characteristic

$$\frac{dp}{dt} = u \pm a \tag{3.4}$$

with compatibility equation (see eqn 3.5)

$$\frac{dp}{dt} = \pm \rho a \frac{du}{dt} \tag{3.5}$$

Similarly along a curve of slope of the particle

$$\frac{dx}{dt} = u \tag{3.6}$$

with compatibility equation (see eqn 3.7)

$$\frac{dp}{dt} = a^2 \frac{d\rho}{dt} \tag{3.7}$$

In order to obtain a wave pattern solution with time, boundary conditions are required which relate the conditions outside the pipe with those inside (subroutines are derived in Ref 6). For this method of solution, it is convenient to convert the thermodynamic variables ρ and p to a and a_{ref}.

3.2 The Non Dimensional Characteristic and Riemann Variables

In the previous paragraphs, the physical interpretation of results has been in terms of pressure and velocities. A direct representation of pressure can be obtained for hometropic flow if the velocities are divided by reference speed of sound, a_{ref}.

Similarly non dimensiolization is extended to distance x and time t by introducing a reference length, L_{ref}.

Thus, $A = \frac{a}{a_{ref}}$; $U = \frac{u}{a_{ref}}$; $X = \frac{x}{L_{ref}}$; $Z = \frac{a_{ref}}{L_{ref}} t$

The original characteristic equations (sect 3.1) were

$$\frac{dx}{dt} = u \pm a \tag{3.8}$$

and $$\frac{da}{du} = \mp \frac{\gamma - 1}{2} \tag{3.9}$$

In non dimensional form these become

$$\frac{dX}{dZ} = U \pm A \tag{3.10}$$

$$\frac{dA}{dU} = \mp \frac{\gamma - 1}{2} \tag{3.11}$$

and $$A = \frac{a}{a_{ref}} = \left[\frac{p}{p_{ref}}\right]^{(\gamma-1)/2\gamma} \tag{3.12}$$

Consider the expression $\frac{dA}{dU} = -\frac{\gamma - 1}{2}$

Integrating with $A = \lambda$ at $U = 0$ we get

$$\lambda = A + \frac{\gamma - 1}{2} U$$

Thus for λ characteristic

$$\frac{dX}{dZ} = U + A \tag{3.13}$$

$$\frac{dA}{dU} = -\frac{\gamma-1}{2} \tag{3.14}$$

and $$\lambda = A + \frac{\gamma-1}{2}U \tag{3.15}$$

Similarly for β characteristic

$$\frac{dA}{dU} = \frac{\gamma-1}{2}$$

Integrating with $A = \beta$ at $U = 0$ we get

$$\frac{dX}{dZ} = U - A \tag{3.16}$$

$$\frac{dU}{dA} = \frac{\gamma-1}{2} \tag{3.17}$$

and $$\beta = A - \frac{\gamma-1}{2}U \tag{3.18}$$

Note that λ is constant along λ characteristic; the same for β. From equations (3.15) and (3.18) we get

$$A = \frac{\lambda + \beta}{2} \text{ and } U = \frac{\lambda - \beta}{\gamma - 1}$$

For convenience let $$a = \frac{3-\gamma}{2(\gamma-1)} \tag{3.19}$$

and $$b = \frac{\gamma+1}{2(\gamma-1)} \tag{3.20}$$

Thus from equations (2.19) and (2.20) we have for λ characteristic

$$\left(\frac{dX}{dZ}\right)_{\lambda} = b\lambda - a\beta \tag{3.21}$$

Similarly for β characteristic

$$\left(\frac{dX}{dZ}\right)_{\beta} = a\lambda - b\beta \tag{3.22}$$

Let $\lambda = \lambda_I$ for positive x-axis from left to right

$\lambda = \lambda_{II}$ for positive x-axis from right to left

i.e $$U = \frac{\lambda_I - \lambda_{II}}{\gamma - 1} \tag{3.23}$$

$$A = \frac{\lambda_I + \lambda_{II}}{2} \tag{3.24}$$

For the λ slope, $\lambda = \lambda_I$ and $\beta = \lambda_{II}$

Thus $\left(\frac{dX}{dZ}\right)_{\lambda_I} = \frac{\gamma+1}{2(\gamma-1)}\lambda_I - \frac{3-\gamma}{2(\gamma-1)}\lambda_{II}$ (3.25)

Similarly for λ_{II} slope we have $\lambda=\lambda_{II}$ and $\beta=\lambda_I$

Thus $\left(\frac{dX}{dZ}\right)_{\lambda_{II}} = \frac{3-\gamma}{2(\gamma-1)}\lambda_{II} - \frac{\gamma+1}{2(\gamma-1)}\lambda_I$ (3.26)

where λ_I and λ_{II} are commonly known as Riemann Variables. Equations (3.25) and (3.26) are the basis for the main program for the engine simulation.

3.3 Numerical Solution of the Characteristic Equations

The numerical solution of the characteristic equations is performed wholly in the position diagram, i.e X-Z field using rectangular mesh which gives time history of variable at a fixed location.

The procedure is that the grid pattern is fixed in the X-direction but the Z-coordinate of the grid lines are adjusted according to the stability criterion (sect 3.3.1) for the numerical solution of quasi-linear hyperbolic partial differential equations. The regular pattern of rectangles are fixed by the fact that the grid proportions $\Delta Z:\Delta X$ are fixed at each time interval, ΔZ. At any time $Z=Z1$, Riemann's variables λ_I and λ_{II} are evaluated at each mesh point. The time interval ΔZ for the next time step is evaluated from λ_I and λ_{II} at time Z. The next time $Z=Z1+\Delta Z$ is then determined and the procedure repeated.

3.3.1 Stability Criterion

The mesh proportions are selected such that $\frac{\Delta Z}{\Delta X} = \frac{1}{|U|+A}$

This means that the mesh proportions will vary throughout the flow field in the Z-X diagram. In practice the procedure is to fix the length ΔX and allow ΔZ to vary in each time step. Under this condition the values of A and U are determined at each mesh point and ΔZ is selected for the minimum value of $\Delta X/(|U|+A)$. At any time step Z, the values of λ and β at each mesh point are evaluated from the previous values of λ and β.

Thermodynamic quantities are then evaluated from λ_I and λ_{II} using the relationship:

$$\left(\frac{p}{p_{ref}}\right)^{(\gamma-1)/2\gamma} = \frac{\lambda_I + \lambda_{II}}{2} \quad (3.27)$$

$$\text{and} \quad \frac{u}{a_{ref}} = \frac{\lambda_I - \lambda_{II}}{\gamma - 1} \quad (3.28)$$

3.4 Program Organization

The computer solution of the previous section is organized in such a way that it caters for the subroutines which deal with the boundary conditions. The calculations in these routines determine conditions at all interval mesh points of the duct section. At the duct ends, the boundary equations are used in conjunction with the wave equations to establish the values of λ and β. Depending upon a particular engine, the form of the boundary conditions will vary widely. The program structure has therefore arranged so that

the calculation of the quantities λ and β is carried out at separate boundary operations. In this way, only boundary conditions of particular interest to the problem at hand need be included in the program.

The master program portion is principally concerned with the organization of the data describing a particular engine under investigation and with printing information about the solution.

3.4.1 Program Input Data

Data read into this segment (Appendix A) describe the engine under investigation in terms of engine geometry, valve area, cylinder pressure and temperature when the inlet valve opens. The thermodynamic quantities p and T are converted into λ and β values and stored in mesh arrays. For each boundary calculations the known values of λ and β at the boundary mesh points of each duct section are then used to transfer the collected information to the boundary routines for subsequent calculation of λ and β values.

4 0 Air Flow Measurements

4.1 Air Flow Rate

Air flow measurement at particular steady state speed of the engine is achieved by using a perplex orifice whose discharge coefficient is known in advance (Cd = 0.95). Air pulsations during induction process is suppressed by passing the air through a box containing baffles. Inclined manometer is connected to the air box to indicate the intake pressure. The experiment was done under three different engine speeds (1300, 1580 and 2090rpm). Thus the experimental mass flow rate is given by:

$$\dot{m}_a = Cd\ A \sqrt{2\ \rho_a\ g\ H\ \rho_w} \qquad (4.1)$$

where Cd = nozzle discharge coefficient
A = nozzle cross section area (= pipe diameter)
ρ_a = air density
g = gravitational acceleration
H = manometric reading height
ρ_w = water density

4.1.1 Experimental Volumetric Efficiency

Evaluation of experimental efficiency is based on the ideal mass of air consumed per engine cycle. The ideal mass flow rate is given by:

$$\dot{m}_t = \frac{N}{2} V_c \rho_a \qquad (4.2)$$

where $\rho_a = \frac{p}{RT}$ = air density
p = ambient pressure
T = ambient temperature
V_c = cylinder volume
N = engine speed

The experimental volumetric efficiency is then calculated from equations (4.1) and (4.2). Thus $\eta_{va} = \frac{\dot{m}_a}{\dot{m}_t}$

4.1.2 Predicted Volumetric Efficiency

Since the evaluation of the improved cylinder filling is expressed in terms of volumetric efficiency, the predicted air flow rate is obtained for the validation of the simulation program. The predicted volumetric efficiency is based on the theoretical (ideal) mass of air consumed per engine cycle. The rate of change of mass, dm/dt in the cylinder at any crank angle position during the inlet valve open is given by;

$$\dot{m} = \frac{dm}{dt} = \rho u A \qquad (4.3)$$

where ρ = gas density
u = gas velocity
A = pipe cross section area

The amount of air in the cylinder at any crank position is obtained by integrating the rate of change of mass from the time the inlet valve opens.

$$m_a = \int_{AVO}^{\theta} \frac{dm}{dt}\frac{dt}{d\theta}\, d\theta \qquad (4.4)$$

But $\omega = \frac{d\theta}{dt}$

$$\text{Thus } m_a = \frac{1}{2\pi N}\int_{AVO}^{\theta} \frac{dm}{dt}\, d\theta \qquad (4.5)$$

The amount of air in the cylinder when the inlet valve closes is obtained by integrating equation (4.3).

$$m_a = \frac{1}{4\pi N}\int_{AVO}^{AVC} \frac{dm}{dt}\, d\theta \qquad (4.6)$$

Hence the predicted theoretical efficiency is given by

$$\eta_{vt} = \frac{m_a}{m_d} \qquad (4.7)$$

where m_d = mass of air that would fill the cylinder swept volume

$$= \rho_a V_c$$

$$= \frac{p_a V_c}{RT_c}$$

4.2 Manifold Tuning

In the discussion, the manifold tuning is based on the Helmholtz resonator theory since it plays a major role in cylinder filing. The tuning frequency relationship[3] is shown below (eqn 4.8).

$$f_o = \frac{a}{2\pi}\sqrt{\frac{2A(CR-1)}{LV_c(CR+1)}} \qquad (4.8)$$

At this frequency (eqn 4.8), the amplitude of the velocity fluctuation is the maximum producing large pressure pulsations in the cylinder. The tuned length is obtained by rearranging the above equation,i.e.

$$L^* = \frac{a^2}{4\pi^2 f^2} \frac{2A}{V_c} \frac{(CR-1)}{(CR+1)} \qquad (4.9)$$

where L^* = tuned length
V_c = cylinder volume
a = acoustic speed
CR = compression ratio
f = engine speed

5.0 Discussion of Results

5.1 Experimental and Predicted Volumetric Efficiency

The results are best evaluated if they are interpreted in terms of volumetric efficiency basis. The predicted efficiencies are evaluated against the corresponding experimental results. Figures 5.1 and 5.2 depict results at various engine speeds. From the figures it is seen that the best results are achieved at engine speed of 1580rpm which is closer to the engine designed speed of 1500rpm. From the experimental point of view it should be pointed out that the most less accurate data within the experiment is probably that concerning the air flow measurement using inclined manometer in conjunction with visual observation.

5.2 Tuned Length

Experimental and predicted tuned lengths are interpolated from Figs 5.1 and 5.2 respectively. The interpolated results, including the Helmholtz resonator model on tuned lengths at various engine speeds are shown in Fig 5.3. The results seem to follow the same pattern of decreasing tuned length with increasing engine speed. The experimental and predicted results agree reasonably well while the Helmholtz resonator model throughout gives higher values of tuned lengths than either of the two.

Effects of diameter of the intake pipe on the volumetric efficiency was carried out on computer. The results are expressed as a function of tuned lengths and engine speeds (Fig 5.4).

6.0 Conclusion

6.1 Application of Simulation Program

With the simulation program in the present form, the engine parameters such as the inlet manifold, and air flow characteristics can be studied systematically by "running" the engine on the computer by varying engine parameters of interest.

Validation of the program has been demonstrated by comparing experimental and predicted volumetric efficiencies which show quite a good agreement especially so at the speed closer to the engine designed speed of 1500rpm.

6.2 Inlet Manifold Tuning

It has been shown theoretically and experimentally that it is possible to achieve a very substantial supercharge in four-stroke cycle engine by proper proportioning of the intake pipes. Tuned lengths obtained by acoustic theory (Helmholtz resonator model) seem to be slightly higher than those obtained either from experiment or computer simulation. On the other hand, effects of pipe length and diameter were observed that:
1)For a given pipe diameter, the higher the engine speed, the

shorter the tuned length.

2)For a given pipe length, the larger the pipe diameter, the higher the engine speed at which the maximum efficiency occurs.

Nomenclature

Symbol	Definition	Units
a	Speed of sound	ms^{-1}
A	Non dimensional speed of sound	-
CR	Compression ratio	-
N	Engine speed	s^{-1}
P	Pressure	Nm^{-2}
U	Non dimensional velocity	-
x	Distance	m
τ	Non dimensional time	-
γ	Ratio of specific heats	-
β	Riemann variable of characteristic moving LHS	
λ	Riemann variable of characteristic moving RHS	
η	Volumetric efficiency	-

References

1)Anthony Ralston and Hebert S Swirf
Mathematical Methods for Digital Computers
John Willey and Sons Inc (1960)

2)Bingham J F
Intake System Design Using Validated Internal Combustion Engine Computer Model C25/87

3)Engelman H W
Design of Tuned Intake Manifold
ASME Diesel and Gas Power Proceedings (1974)

4)Engelman W H
The Tuned Manifold: or Supercharge Without a Blower
ASME Paper 53-OGP-4 (1953)

5)McCracken D and Dorn W S
Numerical Methods and Fortran Programming
John Wiley and Sons (1964)

6)Mtui Peter L
Experimental and Theoretical Study of Inlet Manifold Tuning of a Four-stroke Cycle Engine
MSc Thesis, University of Strathclyde (UK), (1989)

7)Rowland S Benson
Thermodynamic and Gas dynamics of Internal Combustion Engine
Oxford Science Publication (1982)

APPENDIX A

Input Data to the Engine Simulation Program

Group I: Input Data	
Initial pressure in the inlet pipe	1.013bar
Cylinder pressure in the inlet valve open	1.1bar
Cylinder temperature at inlet valve open	473°K
Reference pressure	1.013bar

Number of meshes	12
Ratio of specific heats	1.4
Ambient pressure	1.013bar
Ambient temperature	295°
Engine speed	(variable)
Group II: Input Data (Specific to the Engine)	
Air valve open after TDC power stroke	355.5°
Cycle of operation	4 (stroke)
Cylinder diameter	0.08m
Stroke length	0.11m
Connecting rod length	0.22m
Inlet pipe diameter	0.03m
Inlet pipe length	0.745m
Nominal compression ratio " "	16.5
Number of points on the area curve	245
Angle from opening including zero degree	220°
Valve area	(variable)
Group III: Output Data	
Number of output locations	1
Location expressed in mesh points	2
Duration of run in degrees crank angle	720°

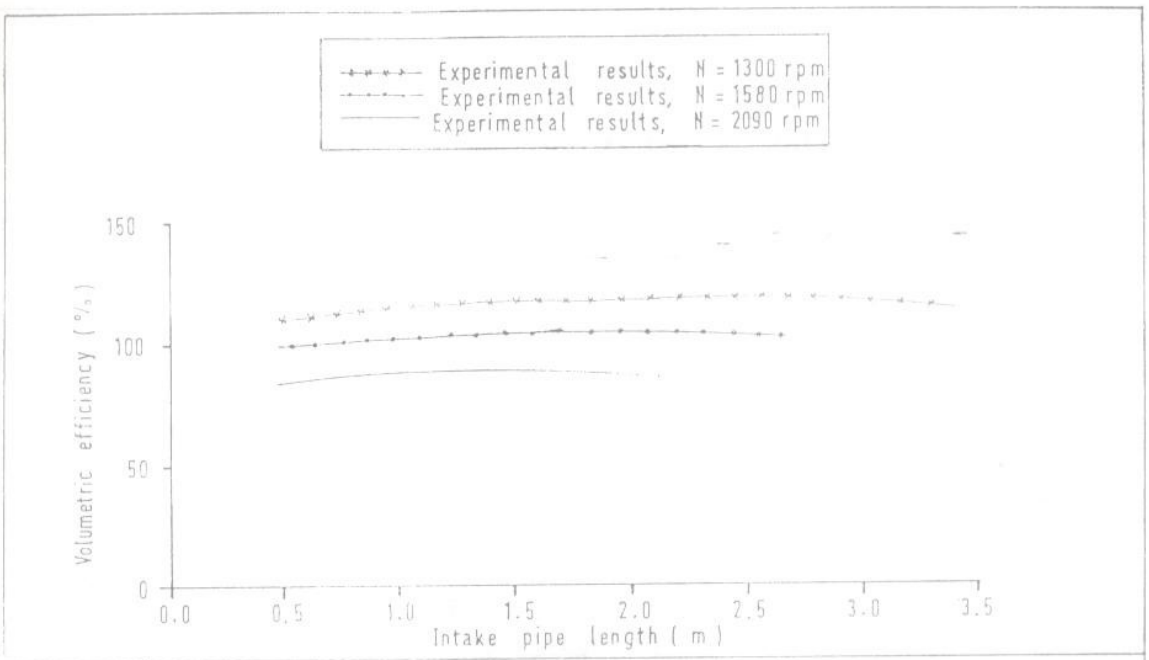

Fig 5.1 Experimental volumetric efficiency at various engine speeds

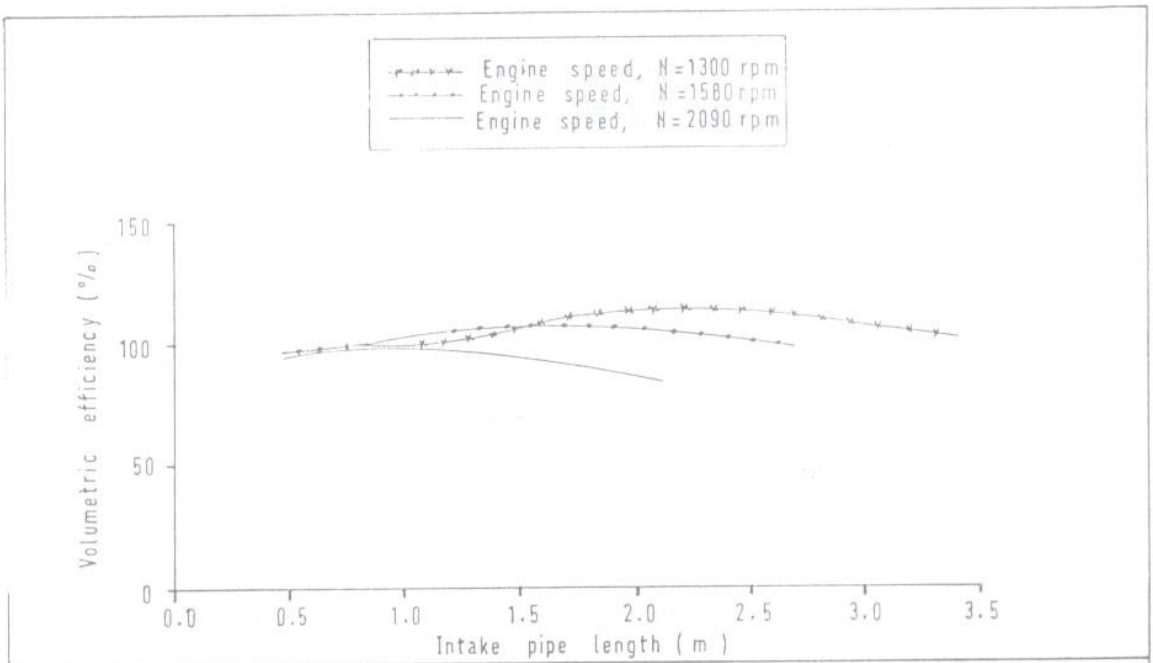

Fig 5.2 Predicted volumetric efficiency at various engine speeds

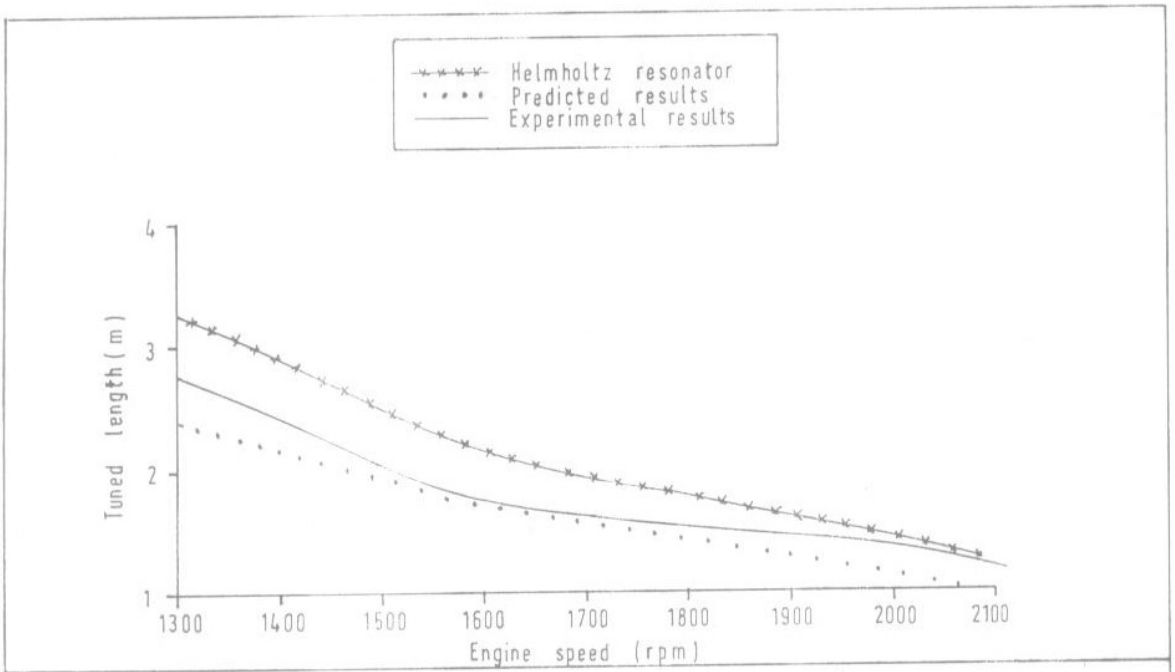

Fig 5.3 Tuned manfold length at various engine speeds (dia = 30 mm)

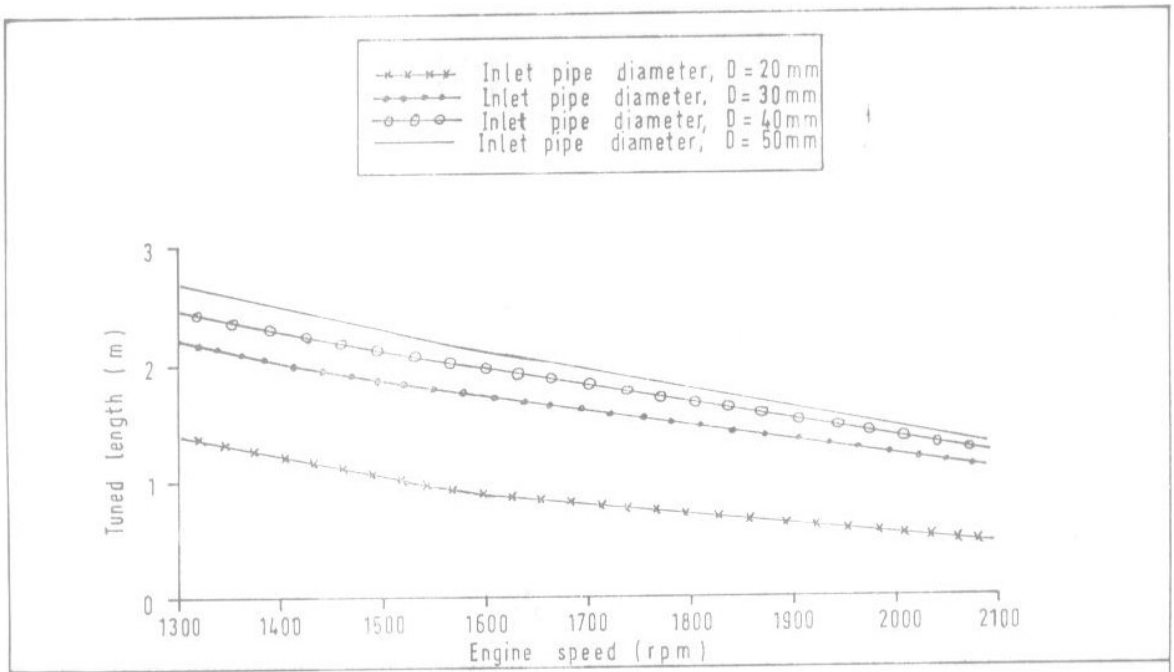

Fig 5.4 Predicted tuned manfold length at various intake pipe diameters